A Minimally Actuated Hopping Rover for Exploration of Celestial Bodies

Eric Hale, Nathan Schara, Joel Burdick
Mechanical Engineering
California Institute of Technology
Pasadena, California 91125

Paolo Fiorini
Jet Propulsion Laboratory
California Institute of Technology
Pasadena, California 91109

Abstract: *This paper describes a minimalist hopping robot that can perform basic exploration tasks on Mars or other moderate gravity bodies. We show that a single actuator can control the vehicle's jumping and steering operations, as well as the panning of an on-board camera. Our novel thrusting linkage also leads to good system efficiency. The inherent minimalism of our hopping paradigm offers interesting advantages over wheeled and legged mobility concepts for some types of planetary exploration. The paper summarizes the evolutionary development of the system, issues relevant to the design of such jumping systems, and experimental results obtained with system prototypes.*

1 Introduction and Motivation

With the recent success of the Pathfinder mission to Mars [10], there is an increasing interest in robotic exploration of Mars and other celestial bodies such as moons, asteroids, and comets. These bodies are characterized by a low to medium gravitational environment. The space exploration community has spent considerable effort and has significant ongoing interest in the development of mechanical mobility systems that are capable of supporting long-range scientific exploration of such bodies.

The most successfully deployed paradigm, as seen in the Pathfinder mission's Sojourner vehicle [10], is a multi-wheeled rover. This concept is currently being extended to both larger and smaller sized rovers. Most 6-wheeled rover designs can traverse obstacles that are at most about 1.5 times their wheel diameter. Inflatable wheels may be able to overcome somewhat proportionally larger obstacles. Smaller rovers can be effectively used in tandem with larger rovers to increase exploration range, in spite of their limited size, by exploring difficult areas, such as mountain cliffs, in a tethered configuration. Legged rovers have previously been proposed for Lunar and Martian exploration [1] in order to overcome the limited traversability of wheeled vehicles in rugged terrain.

These approaches to surface mobility have two significant drawbacks. First, even exotic types of wheeled rovers can only drive over obstacles that are at best a fraction of the vehicle's body length. Thus, some terrains are not accessible to wheeled vehicles. While legged robots can potentially access rough terrains, they are mechanically complex, requiring numerous joints, actuators, and linkages. Even wheeled rover vehicles use a significant numbers of actuators and complex suspension linkages. For example, the Sojourner mobility system used 10 motors, while prototypes for the 2005 Mars mission have 12 independent actuators [17]. Hence, most actively explored paradigms for planetary mobility are based on a large number of actuators. There are a number of obvious drawbacks to using many motors and their associated linkages: an inherent risk in system failure; a need for larger power supplies and/or solar cells; a need for complex power electronics; and increased system weight (which reduces the weight that can be allocated to science payloads).

Reducing the number of actuators is an attractive goal for planetary rover design, since such designs are like to be smaller and lighter, with lower risk of failure. Furthermore, with significantly reduced size/mass, there is a greater likelihood that several such rovers could be deployed in a single rocket launch payload. However a truly minimally actuated device may not have the functionality necessary to carry out meaningful tasks. The research presented in this paper explores the trade-offs between functionality and complexity in the context of the design and development of a single-actuator hopping robot, capable of moving a camera and a small science package by jumping. Our hopper's operation, which is described below, is more akin to the movement of a frog, rather than the oscillatory behavior of typical hopping robots [12]. We show that a single actuator is enough to propel, steer, and self-right a simple hopper. The same actuator can also pan an on-board camera as well as manage a science package. Furthermore, the entire system weighs less

than 1.5 Kg, and efficiently converts stored energy to hopping motion. Hence, our single actuation design offers surprising capability, compactness, and efficiency.

Obviously, our limited actuation hopper cannot have all of the functionality of a wheeled or multi-legged vehicle. However, our work suggests that these jumpers may be a useful addition to the planetary rover family (in fact, they may operate in tandem with conventional rovers). They may be well suited for the cooperating behaviors planned for the next phases of Mars exploration, wherein many simple exploratory devices will coordinate their motions to collectively gather distributed scientific data over large areas.

After summarizing relevant prior work below, Section 2 describes the goals and issues that constrained our development, while Section 3 describes the first ("generation one") prototype. Section 4 summarizes the performance of this system and its shortcomings. The lessons learned from this system led to the second generation system, whose design and performance are described in Sections 5 and 6.

Relation to Prior Work. Hopping systems for planetary mobility were first proposed in Ref.s [11, 14] as a promising transportation concept for astronauts in a Lunar environment. A first order analysis of Lunar hopper performance is presented in Ref. [6]. The authors propose a single-seat device propelled by a gas actuated leg hinged under the astronaut seat and stabilized by four elastic legs. Automatic reorientation of the hopper is not supported in this design concept. A two-seat hopping laboratory which is capable of changing direction during the stance phase is also briefly discussed. Based on data from the Apollo missions, the paper also compares different approaches to Lunar transportation, showing that hopping is an efficient form of transportation in a low-gravity environment. More recently, a hopping robot, whose structure is the precursor for some aspects of our first generation device, is described in [9]. The common characteristic of these two hopping systems is motion discontinuity, since a pause for reorientation and recharge of the thrust mechanism is inserted between jumps. The systems described in this paper have a similar characteristic.

Laboratory demonstrations of hopping robots have generally focused on continuous motion and dynamic stability, without pauses between jumps. Raibert's seminal work in this area is summarized in [12], and analyzed mathematically in several works, such as Ref.s [7, 8, 13]. In contrast to our design, these hoppers required several actuators for propulsion and stabilization. Research on non-holonomic systems has motivated a renewed interest in the control of hopping robots. An often analyzed device is the "Acrobot", a reversed double-pendulum with a single actuator located in the joint and free to move its base [2, 3, 5, 16]. Ref. [2] describes how to make the Acrobot jump by accelerating its center of mass until the base loses ground contact. The Acrobot's landing attitude is controlled by compensating for the robot's non-zero angular momentum at lift-off with in-flight rotations of the lower link. While the acrobot uses only one actuator, it is only capable of motion on the vertical plane. In contrast, our single motor hopper is not restricted in its motions.

An earlier prototype of the first generation rover described in Section 3 is presented in more detail in Ref. [4]. We briefly summarize this system for a few reasons. First, we report on experimental results that were not presented in Ref. [4]. Second, some of the computing, electrical, and sensing subsystems are the same in both generations, and thus need only be discussed once. Most importantly, lessons learned from and evaluation of this system motivate the improved version described in Section 5, and provide some general lessons for the design of jumping vehicles.

2 General Design Goals and Operating Assumptions

Our design and development program is driven by the desire to: (1) minimize the total number of system actuators; (2) minimize the overall size and weight of the entire package so that multiple rovers can be deployed; (3) carry a television camera and some simple on-board scientific sensors; and (4) achieve sufficient mobility to realize some useful scientific capabilities. The system should be able to carry enough on-board energy storage, combined with solar-cell assistance, to enable a useful mission lifetime of weeks or months. Hence, energy efficiency must be of some concern.

The hopper must operate in terrain that ranges from sand to hard rock, and whose topography is unpredictable and varied. The mechanism must achieve a statically stable, steady-state posture between jumps for the purposes of camera image acquisition and scientific measurements. We assume that the vehicle is operating in a moderate gravitational environment, such as Mars (where gravity is about 1/3 that of earth). Microgravity environments (such as on asteroids) present additional complications, as the hopper may exceed escape velocity during lift off. "Micro" wheeled rovers have been proposed for such environments [18].

The simultaneous control of hopping height, hopping direction, hopper stability, and camera pointing would require several actuators. To reduce the number of on-board actuators, we forced as many operations as possible to happen sequentially, instead of simultaneously. The hopper's operational cycle was broken down

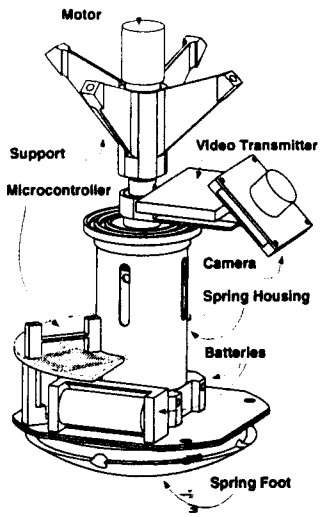

Figure 1: Schematic drawing of the 1^{st} generation mechanism. The surrounding polycarbonate shell is omitted for clarity.

into the following actions: (1) self-right the hopping mechanism after landing; (2) pan the camera to acquire images; (3) deploy scientific instruments as necessary; (4) recharge the thrusting mechanism (in preparation for a jump); (5) point the hopper in the desired direction; (6) jump (release stored energy); (7) go to step (1). As shown below, this sequence may implemented in various ways and with different mechanisms.

3 The First Generation Design

Fig. 1 depicts the essential internal components of the first generation design. A clear polycarbonate shell surrounds the mechanism, and is attached to the body at the upper support and lower plate, as is shown in Fig. 2. Control of the vehicle by a single actuator is implemented with the aide of an over-running clutch. With the decoupling action of the clutch, rotation of the motor in one direction drives the leg compression and leg release subsystem, while rotation in the other direction drives the camera rotation. Fig. 3 schematically depicts the relative phasing and motor rotations for each operation described below.

Vertical hopping motions are generated by the release of a simple linear spring, which is compressed after each jump via a ball screw that is driven by the motor. The spring housing consists of two concentric cylinders that guide the spring's compression/decompression. The compressed spring is held in place by a spring-loaded ball bearing lock-release mechanism [4]. This mechanism locks after a fixed amount of spring compression is reached. A few extra motor rotations beyond the locking point causes the mechanism to release. By reversing the motor rotation, a camera can be rotated so as to take images through the clear

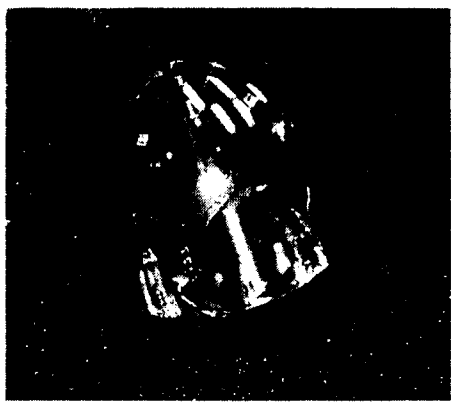

Figure 2: Photograph of the 1^{st} generation system.

shell. The orientation of the body can also be modified by rotating the camera, whose off-axis center of mass causes the vehicle to tilt. Steering is achieved via this concept by tilting the vehicle in the desired direction prior to launch. The self-righting capability is implemented passively in this design by creating a low center of mass—all of the batteries and heavy components are concentrated in the "bottom" of the hopper. •

The electronic subsystem consists of a microcontroller board that is comprised of a PIC CMOS microprocessor, motor controller and power circuits, communication ports, and analog/digital signal acquisition. The board consumes $\sim$ .35 Watts, excluding motor and science instruments. Additionally, the major board components have power-down features to conserve energy. Power is provided by four 12 V batteries. The video micro-camera broadcasts images on channel 14 by an RF transmitter.

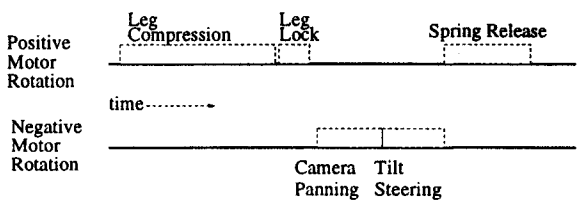

Figure 3: Relative timing of the operations driven by the primary motor.

4 First Generation Post-Mortem

A number of tests were performed to assess this first design. We first focus on its jumping ability, and then summarize other important observations. Even after experimental optimization of the thrust spring, this prototype only realized vertical jumping heights of about 80 cm and horizontal leaping distances of 30-60 cm. We determined that most of energy that was stored in the spring was not converted to motion during the launching process. Let η be the "theoretical

conversion efficiency" of a hopper that is propelled by decompression of an elastic member:

$$\eta = \frac{\text{hopper kinetic energy at takeoff}}{\text{energy stored in compressed member}} \times 100\% .$$

This number assesses how well a given hopping system converts elastic energy stored in the compressed member into actual hopper motion. The kinetic energy at lift-off can be easily be inferred by the realized hopping height and distance. The stored energy is computed from the spring's compression and stiffness constant.

Our experiments showed that the hopper achieved only a 20% efficiency. I.e., 80% of the energy stored in the spring was not converted into hopper motion. Clearly, such an energy loss is unacceptable for space missions. A large number of factors, such as internal dissipation of the spring material as well as friction in the moving and locking mechanisms, each contributed to this dissipation. However, three factors dominated the losses. First, at the end of decompression phase, the foot abruptly stops in an elastic impact with a mechanical stop, thereby dissipating its kinetic energy. The magnitude of this loss is proportional to the ratio of foot' mass to total mass. In this design, the loss equals 15% of the spring's stored energy. Clearly, one should always reduce the foot's mass to minimize this loss.

To understand the other factors, note that the total energy realized by leg decompression during lift-off is:

$$E = \int_{t_i}^{t_{off}} F_R \cdot V_h \, dt \qquad (1)$$

where F_R is the wrench on the hopper due to realized leg thrust, V_h is velocity of the hopper's center of mass. Spring decompression starts at time t_i, and the hopper breaks ground contact at t_{off}. For a lossless linear spring, $F_R = k_l \Delta x$, where k_l is the spring constant and Δx is the deviation from the unsprung length. In reality, F_R is reduced by loss mechanisms. Because the hopper tilts in order to steer, the ground reaction force is often not normal to the surface, and may falls outside the Coulomb friction cone. In this case, slippage and energy loss occurs during take-off. The horizontal component of F_R is bounded by the Coulomb law. Eq. (1) says that the more the leg thrust force exceeds the Coulomb limit, the greater is the percentage energy loss. Such slipping was observed in our trials.

While the losses outlined above are obvious, the following one is more subtle, and involves an inherent problem in the use of linear springs for hopping. Consider the behavior of Eq. (1) during the decompression phase of the simple model in Fig. 4(a). In the model, let M be hopper mass and k_l the leg stiffness. Ground compliance is crudely modelled with a spring of stiffness k_g. First consider the case of solid ground:

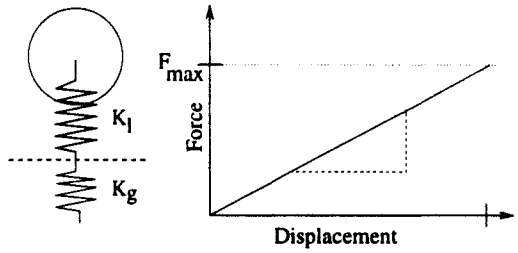

Figure 4: (a) simplified model; (b) Reaction Force vs. leg displacement for Generation 1 thrust spring.

$k_g \to \infty$. If $x(t)$ denotes vertical displacement of the hopper's center of mass from the ground plane, a simple analysis shows that:

$$x(t) = l_0'(1 - \cos(\omega t))$$

where $l_0' = l_0 - Mg/k_l$ and $\omega = \sqrt{k_l/M}$. Here g is the gravitational constant and l_0 is the amount of spring compression at thrust onset. Neglecting frictional and other losses summarized above, substitution of $F_R = k_g(l_0 - x(t))$ and $V_h = \dot{x}(t)$ into Eq. (1) yields the kinetic energy delivered to the hopper by the leg thrust:

$$E(t) = \frac{k_l (l_0')^2}{4}[1 - \cos(2\omega t)] . \qquad (2)$$

In the idealized case, the hopper will lift off when $x(t_{off}) = l_0'$, i.e., when $t_{off} = \frac{\pi}{2\omega}$. At this idealized lift-off time, Eq. (2) yields the expected result that all of the spring's potential energy is converted into kinetic energy. Fig. 5 plots Eq. (2) vs. time during the lift off phase. Note that more of the kinetic energy is realized during the latter part of the decompression cycle. I.e., while F_R assumes a large value at the beginning of lift off, V_h is small. Consequently, the integrand of Eq. (1) is initially small.

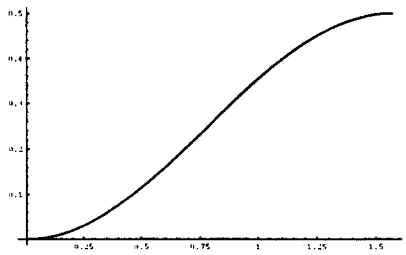

Figure 5: Plot of realized kinetic energy (in units of $k(l_0')^2$) vs. time for idealized linear spring ($\omega = 1$).

Should the hopper prematurely leave the ground before the spring is fully extended, part of the spring's stored energy will not be converted to kinetic energy. In fact, Fig. 5 implies that *premature lift-off* is particularly bad for linear springs, where more of the useful work is realized near the end of the decompression cycle. A more sophisticated analysis of this problem, which includes the ground compliance and the nonlinear coil spring phenomena known as *surge* [15], suggests that the linear spring will often experience premature

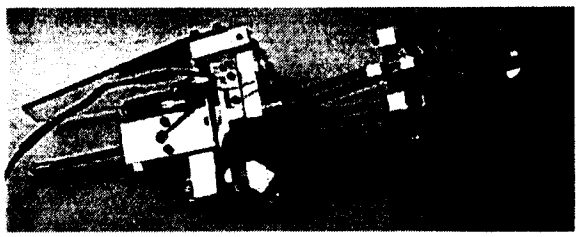

Figure 6: Side view of uncompressed 2^{nd} Generation hopper. The outer shell is removed for clarity.

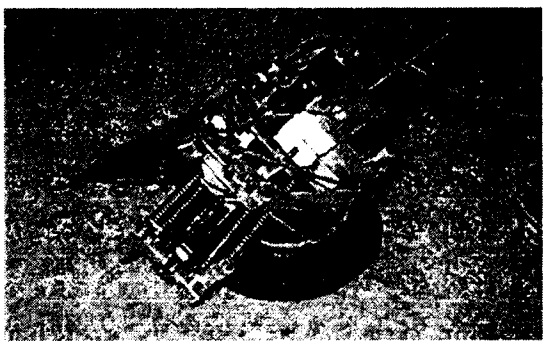

Figure 7: Photo of 2^{nd} Generation hopper in compressed state. The outer shell is removed for clarity.

lift-off, thereby limiting the conversion of stored energy to hopping motion. Moreover, the more that F_R exceeds Mg at the beginning of the thrust, the greater is the likelihood of premature lift-off.

Fig. 4 also suggest another deficiency in the linear spring design. The motor's peak design torque is determined by the spring force at maximum compression. Given the discussion above, we can conclude that most of the motor's design torque is required to compress the spring in a regime where it does little good.

Besides inefficiency, the first generation design had these drawbacks: (1) the passive self-righting system will clearly not work in many terrains, and is therefore not robust; (2) the steering system was not reliable.

5 The Second Generation Design

The goal of the second generation design was to solve the three major shortcomings of the first generation system: (1) inefficient hopping; (2) unrobust steering; (3) unrobust self-righting capability. We were able to realize all of these objectives while still using only a single actuator. As seen in Figs. 6 and 7, the design and construction of this device is considerably more complicated than that of the first generation. Hence, the following discussion is broken down by subsystem.

Jumping mechanism. The need for improved energy conversion efficiency lead us to consider different means for storing and releasing mechanical energy. While we considered gas expansion, linear impulsive actuators, and other exotic means to store and release energy, we concluded that mechanical springs were a convenient and robust storage mechanism. To solve the inefficiency problem, we turned to a combined spring/linkage mechanism. Fig. 8 depicts the geometry of a geared 6-bar spring/linkage system that we have found to be effective. Fig. 9 shows a photograph of its mechanical implementation. The leg extension is along the y-direction in Fig. 8. Displacements in the y-direction induce, through the linkage, displacements in the linear spring. In effect, the linkage creates a nonlinear spring from a linear spring. In addition, this concept can be practically implemented in a stiff structure with low internal friction.

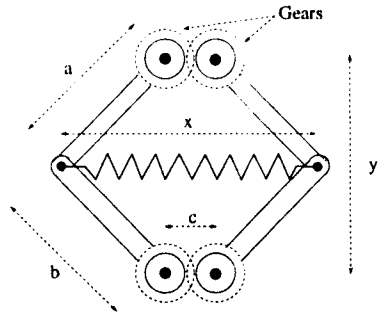

Figure 8: (a) The 2^{nd} generation energy storage linkage, a 6-bar geared mechanism.

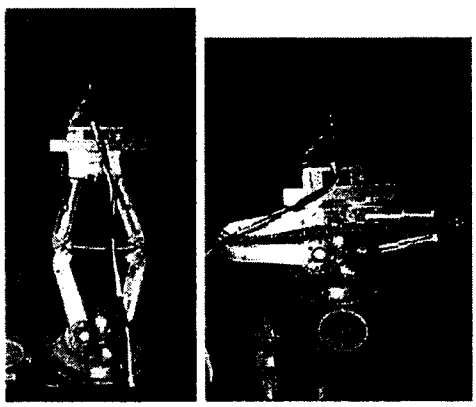

Figure 9: (a) Photo of 2^{nd} generation thrust leg: (a) uncompressed; (b) compressed state. The self-righting mechanisms and outer shell are removed for clarity.

The thrust force versus leg displacement relation for this mechanism can be determined as follows. From the geometry of Fig. 8 one can easily derive an expression for y as a function of x:

$$y = \sqrt{a^2 - (x-c)^2/4} + \sqrt{b^2 - (x-c)^2/4}. \quad (3)$$

This equation can be solved for x:

$$x = c + \frac{\sqrt{2a^2(b^2+y^2) - (b^2-y^2)^2 - a^4}}{y} \quad (4)$$

If F_x denotes the spring force along the x-axis due to spring distension, and if F_y is the thrust force in the

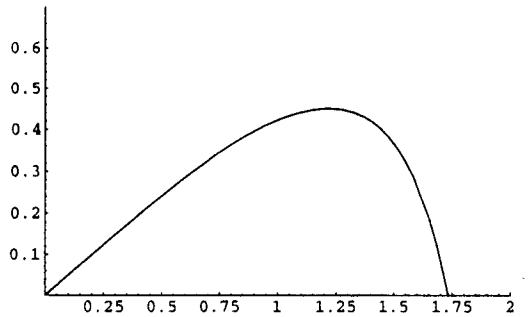

Figure 10: Reaction Force vs. leg extension for the 6-bar geared linkage (case $a = b$).

y-direction, then the principle of virtual work states that for an infinitesimal displacement of the mechanism, $F_x\ dx = F_y\ dy$. From this we obtain:

$$F_y = \frac{F_x}{dy/dx} = \frac{-k(x-l_0)}{dy/dx}$$

$$= \frac{4k(x-l_0)}{x-c}\left[\frac{\sqrt{a^2-\frac{(x-c)^2}{4}}\sqrt{b^2-\frac{(x-c)^2}{4}}}{\sqrt{a^2-\frac{(x-c)^2}{4}}+\sqrt{b^2-\frac{(x-c)^2}{4}}}\right] \quad (5)$$

where k and l_0 are respectively the spring's constant and undistorted length. An expression for F_y as a function of y can be obtained by substituting Eq. (4) into Eq. (5). For the particular case where $a = b$ (which represents our prototype),

$$F_y = k\ y\left[\frac{(c-l_0)+\sqrt{4a^2-y^2}}{\sqrt{4a^2-y^2}}\right].$$

Fig. 10 plots F_y vs y for the case where $a = b$, $(l_0 - c) = 1$, and the spring constant is normalized, $k = 1$.

The utility of this linkage can be understood by comparing the shape of this graph with that of Fig. 4(b). The maximum leg thrust is realized in the middle of the thrusting phase, while the thrust force at the onset of lift-off is quite low. This force/displacement profile substantially reduces the likelihood of premature lift-off. Furthermore, since the peak force realized during displacement is reduced, the motor's peak design torque is reduced as compared with the linear spring leg. This allows a small motor to recharge the thrust mechanism. Experiments with this system verified these observations: this leg realized a 70% conversion efficiency, versus 20% for the first design.

Mechanically, the primary motor compresses the leg via a power screw. The screw is driven until it connects with a latching mechanism, whereupon leg compression commences. When the leg is sufficiently compressed, a mating wedge on the 6-bar releases the leg latch. The entire assembly is mounted at a roughly 50 degree angle with respect to the foot's horizontal axis.

Steering Mechanism. To robustly and accurately point this system in a desired direction, as well as to point the on-board camera, the second generation device employs an active steering mechanism. The main robot structure is attached to the foot by a bearing that rotates about the vertical axis (Fig. 11). When the leg reaches its maximum compression, a pinion gear that is driven by the primary motor engages with a ring gear that is rigidly attached to the foot. Rotation of the pinion controls the steering angle and camera panning.

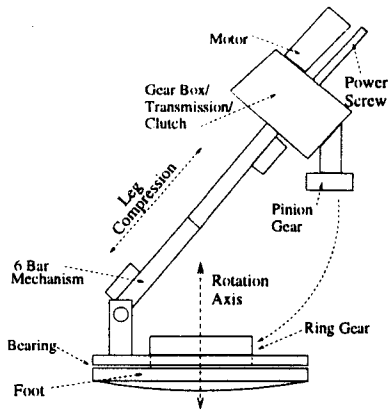

Figure 11: Schematic of steering mechanism. The self-righting mechanism and several components are omitted for clarity.

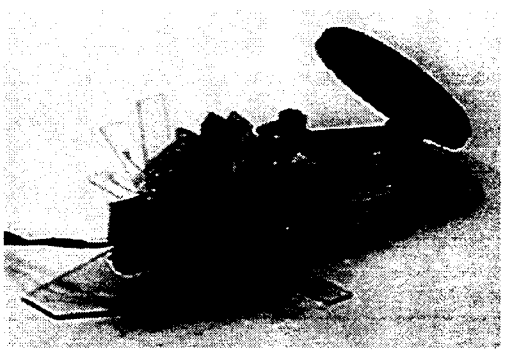

Figure 12: Time elapsed photo showing opening of side flap during Phase 1 of self-righting operation.

Self-Righting Mechanism. The hopper will typically land in an unpredictable toppled configuration. Hence, an active mechanism was devised to bring the mechanism to an upright and stable posture. To cope with a large variety of possible landing configurations, a two stage self-righting process and self-righting mechanism was designed. The outer profile of the uncompressed mechanism is roughly a triangular prism. Hence, the system is very likely to come to rest on one of its faces. During the *first phase* of the self-righting process, flaps (whose stored configurations make up part of two faces) open up, causing the hopper to roll onto its "back" face. A time elapsed photograph of one flap movement is shown in Fig. 12. In the *second phase*, the rotation of a large flap connected to the hopper's

back face forces the hopper toward an upright configuration. The leg compression phase is timed to coincide with this part of the self-righting process, so that the hopper's center of mass sympathetically shifts in way to aid the uprighting process that is driven by the back flap's operation. The leg is essentially compressed by the end of phase II. Mechanically, the coordination is done by driving the Phase II process from the gears of the geared 6-bar leg. With this two phase process, the hopper can nearly always be brought to an upright position, in preparation for the next operational cycle. The hopper's broad foot combined wth its low center of mass in the compressed state ensures that the upright posture is statically stable.

Operation Sequence. The main hopper subsystems were outlined above. A key novelty of our design is its ability to drive all of these subsystems with single motor. Like the first generation design, we use an overrunning clutch to allow opposite motor rotations to drive different operations. However, the second generation design cycles through more operations, and novel timing mechanisms, mechanical logic, and couplers (whose presentation is beyond the scope of this paper) were introduced to coordinate the various actions. Fig. 13 presents a timing diagram like the one in Section 3.

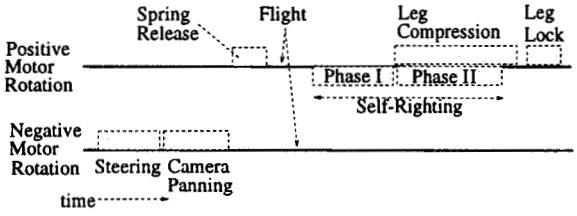

Figure 13: Depiction of Timing/Phase of motor operations driven by the single primary motor.

6 Experimental Results

We tested this device on a variety of surfaces. It typically jumps a horizontal distance of 70-80 inches, and reaches a vertical height of ~35 inches during free-flight. On Mars, one of the primary opportunities for this vehicle, this performance would translate into a horizontal movement of ~ 20-24 feet and vertical ascent of ~9 feet. This system could potentially overcome physical obstacles of considerable size, and that are many times the vehicle's body size.

Fig.s 14 through 18 show digitized images from a video that captures a complete cyle of the hopper's operation. The cycle begins with the robot in a posture like that of Fig. 7. After steering to the intended direction, the leg is released. Fig. 14 shows a blurry image of the device during free-flight. During this particular trial, the device came to rest on its side after touchdown (Fig. 15). Fig. 16 captures an instant during

Figure 14: Flight Phase.

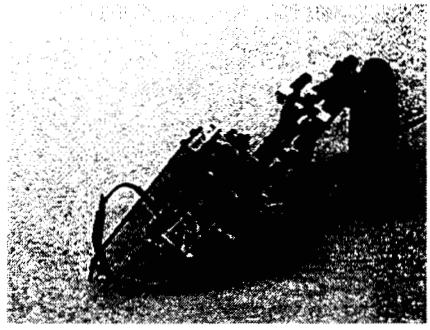

Figure 15: Landing configuration.

the first phase of the self-righting process, where side flaps unfold to position the hopper on its back. Fig. 17 shows that the hopper has rolled onto its back by the end of the first self-righting phase. Fig. 18 occurs near the beginning of the second self-righting phase, while Fig. 19 occurs near the end of this phase. The back flap is pushing the hopper towards a standing position. The progress towards a standing posture is aided by the leg compression, which moves the mass center in a sympathetic manner.

7 Conclusion

Our minimalist hopper offers surprising capability and reasonable efficiency in a small package that contains a single actuator. We hope that this system and its future versions will offer a useful alternative mobility platform for low cost operations in remote terrain. There are clearly several avenues of future work. Our second generation design achieved significant hopping distances, good efficiency, and robust steering. While

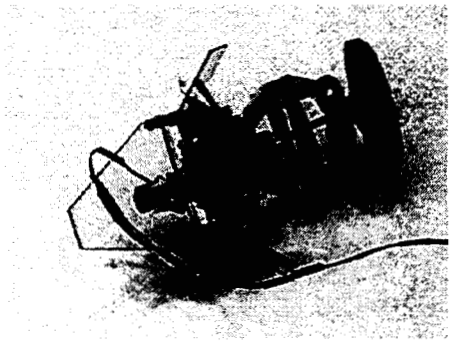

Figure 16: First phase of self-righting sequence. Side flaps are opening.

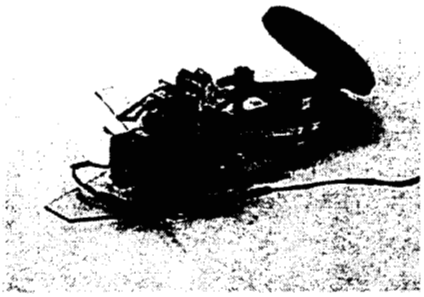

Figure 17: Posture at end of self-righting phase I.

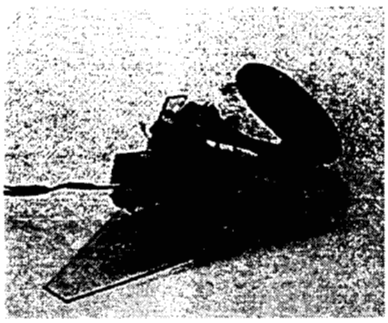

Figure 18: Second phase of self-righting sequence.

it's self-righting ability has been successful in our trials, we currently have no proof that the vehicle can self-right itself in all possible terrains with all possible contact conditions. This is clearly a serious issue that merits further attention. The integration of the on-board computing and power system from the first generation into our most recent prototype is shortly forthcoming. Finally, we need to further investigate and demonstrate solar-cell assisted operation.

Acknowledgments: This research has been carried out in part at the Jet Propulsion Laboratory, California Institute of Technology, under contract with the National Aeronautics and Space Administration.

References

[1] J. Bares, M. Hebert, T. Kanade, E. Krotkov, T. Mitchell, R. Simmons, and W. Whittaker. Ambler: An autonomous rover for planetary exploration. *IEEE Computer*, 22(6):18–26, Aug. 1989.

[2] M.D. Berkemeier and R.S. Fearing. Sliding and hopping gaits for the underactuated acrobot. *IEEE Tran. on Robotics and Automation*, 14(4):629–634, 1998.

[3] A. De Luca and G. Oriolo. Stabilization of the acrobot via iterative state steering. In *IEEE Int. Conf. on Robotics and Automation*, pages 3581–3587, Leuven, Belgium, May 1998.

[4] P. Fiorini, S. Hayati, M. Heverly, and J. Gensler. A hopping robot for planetary exploration. In *Proc. of IEEE Aerospace Conference*, Snowmass, CO, March 1999.

Figure 19: Second phase of self-righting sequence.

[5] J. Hauser and R.M. Murray. Nonlinear controllers for non-integrable systems: the acrobot example. In *American Control Conference*, pages 669–671, 1990.

[6] M.H. Kaplan and H. Seifert. Hopping transporters for lunar exploration. *J. Spacecraft and Rockets*, 6(8):917–922, Aug. 1969.

[7] D.E. Koditschek and M. Bühler. Analysis of a simplified hopping robot. *Int. J. Robotics Reseach*, 10(6):587–605, Dec. 1991.

[8] Z. Li and R. Montgomery. Dynamics and optimal control of a legged roboti in flight phase. In *IEEE Int. Conf. on Robotics and Automation*, pages 1816–1821, Cincinnati, OH, May 1990.

[9] L. Lorigo, C. Paul, R. Brooks, J. McLurkin, and M. Moy. Autonomy for Mars exploration. In *Workshop on Planetary Rovers at IROS'97*, Grenoble, FR, September 7-11 1997.

[10] A. Mishkin, J. Morrison, T. Nguyen, H. Stone, and B. Cooper. Operations and autonomy of the mars pathfinder microrover. In *IEEE Aerospace Conf.*, 1998.

[11] J. Oberth. *The Moon Car.* Harper and Brothers, New York, 1959.

[12] Marc H. Raibert. *Legged Robots that Balance.* The MIT Press, Cambridge, MA, 1986.

[13] M'Closkey R.T. and J.W. Burdick. Periodic motion of a hopping robot with vertical and forward motion. *Int. J. Robotics Reseach*, 12(3):197–218, May 1993.

[14] H.S. Seifert. The lunar pogo stick. *Journal of Spacecraft and Rockets*, 4(7):941–943, July 1967.

[15] J.E. Shigley and C.R. Mischke. *Mechanical Engineering Design.* McGraw-Hill, New York, 1989.

[16] M.W. Spong. The swing up control problem for the acrobot. *IEEE Control System Magazine*, pages 49–55, Feb. 1995.

[17] Rich Volpe. Personal communication. Aug. 1999.

[18] R. Welch, B. Wilcox, and A. Nasif. Nanorover for mars. *Space Technology*, 17(3-4):163–172, April 1998.